Analysis of Axisymmetric Generalized Stoneley Wave in Layered Elastic Solids

B. Yu[a], H. Jing[b,*], J. Wang[b],
Z. Bu[a] and S.A.B. Da Fontoura[c]

[a] *School of Civil & Environmental Engineering and Geography Science, Ningbo University, 818 Fenghua Road, Ningbo, 315211 Zhejiang, China*
[b] *Piezoelectric Device Laboratory, School of Mechanical Engineering and Mechanics, Ningbo University, 818 Fenghua Road, Ningbo, 315211 Zhejiang, China*
[c] *Department of Civil and Environmental Engineering, Pontifícia Universidade Católica do Rio de Janeiro, Rua Marquês de São Vicente 225, 22451-900 Rio de Janeiro, Brasil*

Received: 29.12.2023 & Accepted: 20.02.2024

Doi: 10.12693/APhysPolA.145.247 *e-mail: jinghuimin@nbu.edu.cn

The layered structures of elastic solids have wide applications in various fields of engineering related to natural phenomena, foundations, composite structures, and ultrasonic devices, among others. To have a better understanding of the propagation characteristics of axisymmetric generalized Stoneley waves in a layered structure, the displacement is constructed using the Helmholtz decomposition method with the cylindrical formulation, and then the displacement and stress in the layered structure are presented with potential functions in the wave equations. The transfer matrix method is used to derive the equations of the axisymmetric Stoneley waves in layered elastic solids in the cylindrical coordinates for solutions of wave velocity and amplitudes. With a new formulation in cylindrical coordinates, numerical examples are presented for the dispersion and displacement characteristics of the generalized Stoneley wave of layered solids. The results show that if a low-speed interlayer is added between two semi-infinite media where Stoneley waves do not exist, a wave similar to the Stoneley wave, with displacement decaying exponentially in the semi-infinite direction, can exist. We refer to the Stoneley-like waves that exist in structures with several interlayers between two semi-infinite media as generalized Stoneley waves.

topics: Stoneley wave, transfer matrix, propagation, velocity

1. Introduction

The widely known Stoneley wave is an interface wave that propagates along the interface of two uniform solid half-spaces as the result of the superposition of an inhomogeneous pressure wave (P-wave) and inhomogeneous shear vertical wave (SV-wave). The Stoneley wave has the maximum intensity at the interface and decreases exponentially away from the interface until it eventually vanishes. The Stoneley wave is named after the British seismologist Robert Stoneley, and it has significant applications in seismic exploration and wellbore acoustic logging. The Stoneley waves are most commonly generated during borehole sonic logging and vertical seismic profiling. They propagate along the walls of a fluid-filled borehole. They make up a large part of the low-frequency component of the signal from the seismic source, and their attenuation is sensitive to fractures and formation permeability [1].

Stoneley proved in 1924 that such an interface wave can only be generated when the parameters of the two solid media satisfy a specific condition (the shear wave velocities are almost the same) [2]. It is now known that along an interface between two isotropic half-spaces satisfying the Wiechert condition, which is widely used in geophysical applications, the Stoneley wave may propagate with a velocity that is independent of frequency [3]. Nowadays, it is known that the Wiechert condition is a sufficient but not necessary condition for the existence of the Stoneley wave [4–6].

The description of elastic waves in media with any number of layers usually uses matrix methods, which can be roughly divided into the transfer matrix method and the global matrix method. The transfer matrix method was first proposed by Thomson in 1950 [7]. He introduced a transfer matrix that described the displacements and stresses at the bottom of a layer with respect to those at the top of the layer. Then, through the interlayer boundary conditions, the displacements and stresses at the bottom of the multilayer system are related to those at the top. Haskell improved this method in 1953 [8], so the transfer matrix method is also called the Thomson–Haskell method. However, due to the instability of the transfer matrix method solution when dealing with

large frequency-thickness product [9], Knopoff proposed a global matrix method in 1964 that assembles all interlayer relationships into one matrix. This method has good robustness, but the calculation is slow because of the huge matrix [10].

The analysis of propagation of the Stoneley wave is commonly presented in popular textbooks using the Cartesian coordinate system. However, it can also be extended to other coordinate systems, including the cylindrical coordinate system, to simplify the solution procedure for specific material and structural configurations. For a semi-infinite space, either a Cartesian or cylindrical coordinate system is appropriate for formulating and solving problems concerning wave propagation for the wave velocity and displacements required in applications. Nevertheless, recent studies by our group have shown that the properties and features of waves are dependent on the chosen coordinate system and also show significant differences in the vicinity of the origin [11–13]. As such, the results obtained from different coordinate systems may vary, particularly if the configuration of materials and structures is uncertain or the concern is placed in the wave features near the origin of the coordinate system. In these cases, it is important to obtain both sets of results and verify them using an alternative formulation. This practice is already common in some small-scale critical applications, such as diagnosing eyes and other vital organs in medical treatments. It is therefore necessary to extend such analytical techniques to the analysis of layered structures, which are of particular interest due to their widespread engineering applications with critical functions and circular configurations [14, 15]. Apparently, it is no longer a standard Stoneley wave problem due to the presence of additional elastic layers between two semi-infinite solids, and the generalized Stoneley wave is used to refer to the new problem. It is expected that the formulation and procedure can find properties of waves similar to the Stoneley wave.

2. Analysis of the axisymmetric Stoneley wave in layered solids

For the typical layered structure shown in Fig. 1, the wave propagation is usually analyzed in the Cartesian coordinates, and the equations, methods, and results are dependent on the materials and frequency, or wave velocity, as it is widely known. In general, the Helmholtz decomposition method is utilized to split the displacement vector into two distinct components for a complete representation [16]. With this technique, the first component is the gradient of a scalar potential, which describes the contribution of P-wave. The second component is represented by the curl of a vector potential, reflecting the displacement component of the SV-wave. Referring to the layered solids in Fig. 1

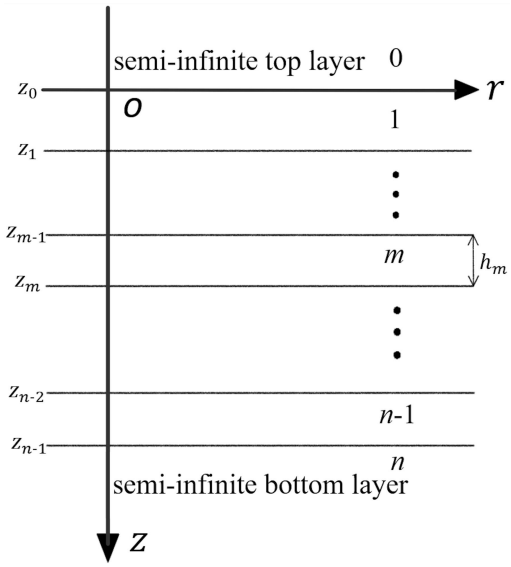

Fig. 1. Horizontally layered solids in cylindrical coordinates.

with cylindrical coordinates, it is assumed that the displacement vector of the axisymmetric cylindrical Stoneley wave, denoted by $\boldsymbol{u}(r,z)$, is expressed as the sum of two components, $\boldsymbol{u}_p$ and $\boldsymbol{u}_{sv}$, which are given by $\nabla\Phi$ and $\nabla\times\boldsymbol{H}_\theta$, respectively, and Φ is a scalar potential and $\boldsymbol{H}_\theta$ is a tangential vector potential. Specifically, the displacement vector now is

$$\boldsymbol{u}\,(r,z)=\nabla\Phi+\nabla\times\boldsymbol{H}_\theta=u_r\boldsymbol{e}_r+u_z\boldsymbol{e}_z, \tag{1}$$

where $u_r\boldsymbol{e}_r$ and $u_z\boldsymbol{e}_z$ are displacement component vectors along the coordinate axes. To simplify the equations and subsequent analysis, a scalar potential function Ψ is chosen as

$$H_\theta=-\frac{\partial\Psi}{\partial r}. \tag{2}$$

Then, with the two potential functions Φ and Ψ, the equations of motion are

$$\begin{aligned}&\left(\frac{\partial^2}{\partial r^2}+\frac{1}{r}\frac{\partial}{\partial r}+\frac{\partial^2}{\partial z^2}\right)\Phi-\frac{1}{c_P^2}\frac{\partial^2\Phi}{\partial t^2}=0,\\&\left(\frac{\partial^2}{\partial r^2}+\frac{1}{r}\frac{\partial}{\partial r}+\frac{\partial^2}{\partial z^2}\right)\Psi-\frac{1}{c_s^2}\frac{\partial^2\Psi}{\partial t^2}=0,\end{aligned} \tag{3}$$

where c_S represents the S-wave velocity and c_P represents the P-wave velocity, respectively.

In this study, we define ω as the angular frequency, k as the wavenumber in the r direction, and c, defined as ω/k, signifies the phase velocity. For the sake of simplicity, $\mathrm{e}^{\mathrm{i}\omega t}$ is omitted throughout the study, where we employ the transfer matrix method in conjunction with cylindrical coordinates for our analysis.

With the cylindrical formulation, the formal solutions of the scalar potentials are given as

$$\begin{aligned}\Phi&=J_0\,(kr)\left(A_1\,\mathrm{e}^{-\mathrm{i}\alpha z}+A_2\,\mathrm{e}^{\mathrm{i}\alpha z}\right),\\\Psi&=J_0\,(kr)\left(B_1\,\mathrm{e}^{-\mathrm{i}\beta z}+B_2\,\mathrm{e}^{\mathrm{i}\beta z}\right),\end{aligned} \tag{4}$$

where $J_0(kr)$ is the zeroth-order Bessel function of the first kind, and A_i and B_i $(i=1,2)$ are unknown amplitudes. The parameters α and β satisfy the following conditions

$$k^2=-\alpha^2+\frac{\omega^2}{c_p^2} \quad \text{and} \quad k^2=-\beta^2+\frac{\omega^2}{c_s^2}. \tag{5}$$

Before presenting a complete solution, let

$$\begin{aligned} &\Lambda(z)=A_1\mathrm{e}^{-\mathrm{i}\alpha z}+A_2\mathrm{e}^{\mathrm{i}\alpha z},\\ &\Omega(z)=B_1\mathrm{e}^{-\mathrm{i}\beta z}+B_2\mathrm{e}^{\mathrm{i}\beta z},\\ &\Theta(z)=k\Omega(z). \end{aligned} \tag{6}$$

Particularly, in the two semi-infinite layers, as shown in Fig. 1, when $z\to\infty$, the potential functions Φ and Ψ must be zero. Therefore, it is required that there is only one term in Λ, Ω and α, β are pure imaginary numbers. That is to say, in the semi-infinite top layer

$$\begin{aligned} &\Lambda_0(z)=A_{01}\mathrm{e}^{-\mathrm{i}\alpha_0 z},\\ &\Omega_0(z)=B_{01}\mathrm{e}^{-\mathrm{i}\beta_0 z},\\ &k\Omega_0(z)=\Theta_0(z), \end{aligned} \tag{7}$$

and in the semi-infinite bottom layer

$$\begin{aligned} &\Lambda_n(z)=A_{n2}\mathrm{e}^{\mathrm{i}\alpha_n z},\\ &\Omega_n(z)=B_{n2}\mathrm{e}^{\mathrm{i}\beta_n z},\\ &k\Omega_n(z)=\Theta_n(z). \end{aligned} \tag{8}$$

As a result, the components of the displacement vector and the components of the stress tensor are now written as follows

$$\begin{aligned} u_r&=\frac{\partial\Phi}{\partial r}-\frac{\partial H_\theta}{\partial z}=-\left[k\Lambda(z)+\frac{\partial\Theta(z)}{\partial z}\right]J_1(kr),\\ u_z&=\frac{\partial\Phi}{\partial z}+\frac{\partial H_\theta}{\partial r}+\frac{H_\theta}{r}=\left[k\Theta(z)+\frac{\partial\Lambda(z)}{\partial z}\right]J_0(kr),\\ \tau_{rz}&=\mu\left(\frac{\partial u_z}{\partial r}+\frac{\partial u_r}{\partial z}\right)=-2k\mu\left[\Lambda'(z)+k\gamma\Theta(z)\right]J_1(kr),\\ \sigma_z&=\lambda\theta_t+2\mu\frac{\partial u_z}{\partial z}=2k\mu\left[k\gamma\Lambda(z)+\Theta'(z)\right]J_0(kr), \end{aligned} \tag{9}$$

where $\gamma=1-\frac{c^2}{2c_S^2}$. The displacement–stress vector is now defined as $\boldsymbol{S}=[U_1,U_2,P_1,P_2]^{\mathrm{T}}$, with

$$\begin{aligned} U_1&=k\Lambda(z)+\Theta'(z),\\ U_2&=k\Theta(z)+\Lambda'(z),\\ P_1&=k\gamma\Theta(z)+\Lambda'(z),\\ P_2&=k\gamma\Lambda(z)+\Theta'(z). \end{aligned} \tag{10}$$

For the convenience of the following notation, we arrange (9) into the following matrix form

$$\begin{bmatrix} u_r\\ u_z\\ \tau_{rz}\\ \sigma_z \end{bmatrix}=J(r)\boldsymbol{S}, \tag{11}$$

where

$$J(r)=\begin{bmatrix} -J_1(kr) & 0 & 0 & 0\\ 0 & J_0(kr) & 0 & 0\\ 0 & 0 & -2k\mu J_1(kr) & 0\\ 0 & 0 & 0 & 2k\mu J_0(kr) \end{bmatrix}. \tag{12}$$

Then let $\boldsymbol{X}=[u_r,u_z,\tau_{rz},\sigma_z]^{\mathrm{T}}$, $\boldsymbol{S}=M\boldsymbol{\Gamma}$, where

$$\boldsymbol{\Gamma}=\begin{bmatrix} k\Lambda(z)\\ k\Theta(z)\\ \Lambda'(z)\\ \Theta'(z) \end{bmatrix}, \quad M=\begin{bmatrix} 1 & 0 & 0 & 1\\ 0 & 1 & 1 & 0\\ 0 & \gamma & 1 & 0\\ \gamma & 0 & 0 & 1 \end{bmatrix}. \tag{13}$$

Consequently, the following system of equations is obtained

$$\begin{aligned} \boldsymbol{S}_T&=M\boldsymbol{\Gamma}_T\\ \boldsymbol{S}_B&=M\boldsymbol{\Gamma}_B\\ \boldsymbol{\Gamma}_T&=G\boldsymbol{\Gamma}_B \end{aligned} \tag{14}$$

The equation system above yields the intra-layer transfer equation of displacement–stress vector

$$\boldsymbol{S}_T=MGM^{-1}\boldsymbol{S}_B, \tag{15}$$

where

$$G=\begin{bmatrix} \cos(\gamma_P kh) & 0 & -\sin(\gamma_P kh)/\gamma_P & 0\\ 0 & \cos(\gamma_S kh) & 0 & -\sin(\gamma_S kh)/\gamma_S\\ \gamma_P\sin(\gamma_P kh) & 0 & \cos(\gamma_P kh) & 0\\ 0 & \gamma_S\sin(\gamma_S kh) & 0 & \cos(\gamma_S kh) \end{bmatrix}, \tag{16}$$

and $\gamma_s=\frac{\beta}{k},\gamma_p=\frac{\alpha}{k}$. In (14) and (15), the subscript T represents the top layer, and B represents the bottom layer. To differentiate between layers, the subscript m is used to represent the m-th layer. At this point, G_m is a matrix that facilitates the transmission of displacements and stresses across the entire structure or from the top to the bottom. Since

$$(\boldsymbol{X}_m)_B=(\boldsymbol{X}_{m+1})_T, \tag{17}$$

it follows that

$$(\boldsymbol{S}_m)_B=R_m(\boldsymbol{S}_{m+1})_T, \tag{18}$$

where

$$R_m = \begin{bmatrix} 1 & 0 & 0 & 0 \\ 0 & 1 & 0 & 0 \\ 0 & 0 & \frac{\mu_{m+1}}{\mu_m} & 0 \\ 0 & 0 & 0 & \frac{\mu_{m+1}}{\mu_m} \end{bmatrix}, \tag{19}$$

and μ_m is the shear modulus of the m-th layer. Thus, from (15) and (18), it is obtained that

$$(\boldsymbol{S}_m)_T = M_m G_m M_m^{-1} R_m (\boldsymbol{S}_{m+1})_T. \tag{20}$$

Furthermore, we define the transfer matrix

$$T(m, m+1) = M_m G_m M_m^{-1} R_m, \tag{21}$$

and then (20) can be written simply as

$$(\boldsymbol{S}_m)_T = T(m, m+1)(\boldsymbol{S}_{m+1})_T. \tag{22}$$

Therefore

$$(\boldsymbol{S}_1)_T = T(1, m)(\boldsymbol{S}_m)_T, \tag{23}$$

where

$$T(1, m) = T(1, 2)T(2, 3)\cdots T(m-1, m). \tag{24}$$

Because

$$(\boldsymbol{X}_0)_B = (\boldsymbol{X}_1)_T, \tag{25}$$

where

$$(\boldsymbol{X}_0)_B = J_0(r)(\boldsymbol{S}_0)_B,$$

$$(\boldsymbol{X}_1)_T = J_1(r)(\boldsymbol{S}_1)_T,$$

$$(\boldsymbol{S}_0)_B = k \begin{bmatrix} 1 & -\mathrm{i}\gamma_{0S} \\ -\mathrm{i}\gamma_{0P} & 1 \\ -\mathrm{i}\gamma_{0P} & \gamma_0 \\ \gamma_0 & -\mathrm{i}\gamma_{0S} \end{bmatrix} \begin{bmatrix} \Lambda_0(z) \\ \Theta_0(z) \end{bmatrix},$$

$$(\boldsymbol{S}_1)_T = T(1, n)(\boldsymbol{S}_n)_T, \tag{26}$$

the expanding of (25) results in

$$\left\{ J_0(r) \begin{bmatrix} 1 & -\mathrm{i}\gamma_{0S} \\ -\mathrm{i}\gamma_{0P} & 1 \\ -\mathrm{i}\gamma_{0P} & \gamma_0 \\ \gamma_0 & -\mathrm{i}\gamma_{0S} \end{bmatrix} \begin{bmatrix} 1 & 0 \\ 0 & k \end{bmatrix} \begin{bmatrix} 1 & 0 & 0 & 0 \\ 0 & 1 & 0 & 0 \end{bmatrix} \right.$$

$$\left. -J_1(r)T(1,n) \begin{bmatrix} 1 & \mathrm{i}\gamma_{nS} \\ \mathrm{i}\gamma_{nP} & 1 \\ \mathrm{i}\gamma_{nP} & \gamma_n \\ \gamma_n & \mathrm{i}\gamma_{nS} \end{bmatrix} \begin{bmatrix} \mathrm{e}^{\mathrm{i}\alpha_n z_{n-1}} & 0 \\ 0 & k\mathrm{e}^{\mathrm{i}\beta_n z_{n-1}} \end{bmatrix} \begin{bmatrix} 0 & 0 & 1 & 0 \\ 0 & 0 & 0 & 1 \end{bmatrix} \right\} \begin{bmatrix} A_{01} \\ B_{01} \\ A_{n2} \\ B_{n2} \end{bmatrix} = \begin{bmatrix} 0 \\ 0 \\ 0 \\ 0 \end{bmatrix}. \tag{27}$$

The existence of a nonzero solution of (27) requires that the determinant of the coefficient matrix be zero, i.e.,

$$\det \left\{ J_0(r) \begin{bmatrix} 1 & -\mathrm{i}\gamma_{0S} \\ -\mathrm{i}\gamma_{0P} & 1 \\ -\mathrm{i}\gamma_{0P} & \gamma_0 \\ \gamma_0 & -\mathrm{i}\gamma_{0S} \end{bmatrix} \begin{bmatrix} 1 & 0 \\ 0 & k \end{bmatrix} \begin{bmatrix} 1 & 0 & 0 & 0 \\ 0 & 1 & 0 & 0 \end{bmatrix} \right.$$

$$\left. -J_1(r)T(1,n) \begin{bmatrix} 1 & \mathrm{i}\gamma_{nS} \\ \mathrm{i}\gamma_{nP} & 1 \\ \mathrm{i}\gamma_{nP} & \gamma_n \\ \gamma_n & \mathrm{i}\gamma_{nS} \end{bmatrix} \begin{bmatrix} \mathrm{e}^{\mathrm{i}\alpha_n z_{n-1}} & 0 \\ 0 & k\mathrm{e}^{\mathrm{i}\beta_n z_{n-1}} \end{bmatrix} \begin{bmatrix} 0 & 0 & 1 & 0 \\ 0 & 0 & 0 & 1 \end{bmatrix} \right\} = 0. \tag{28}$$

Simplifying (28) to a new form

$$\left| \begin{bmatrix} 1 & -\mathrm{i}\gamma_{0S} \\ -\mathrm{i}\gamma_{0P} & 1 \\ -\mathrm{i}\gamma_{0P} & \gamma_0 \\ \gamma_0 & -\mathrm{i}\gamma_{0S} \end{bmatrix} \begin{bmatrix} 1 & 0 & 0 & 0 \\ 0 & 1 & 0 & 0 \end{bmatrix} - R_0 T(1,n) \begin{bmatrix} 1 & \mathrm{i}\gamma_{nS} \\ \mathrm{i}\gamma_{nP} & 1 \\ \mathrm{i}\gamma_{nP} & \gamma_n \\ \gamma_n & \mathrm{i}\gamma_{nS} \end{bmatrix} \begin{bmatrix} 0 & 0 & 1 & 0 \\ 0 & 0 & 0 & 1 \end{bmatrix} \right| = 0, \tag{29}$$

we obtain the dispersion equation of the Stoneley wave in a layered structure.

Next, these equations are further used for displacement calculations. Solving (27) will yield the fundamental solution for the homogeneous equation. The displacements u_r and u_z of the zeroth-layer are

$$\begin{bmatrix} u_r \\ u_z \end{bmatrix} = k \begin{bmatrix} -J_1(kr) & 0 \\ 0 & J_0(kr) \end{bmatrix} \begin{bmatrix} 1 & -\mathrm{i}\gamma_{0S} \\ -\mathrm{i}\gamma_{0P} & 1 \end{bmatrix} \begin{bmatrix} A_{01}\mathrm{e}^{-\mathrm{i}\alpha_0 z} \\ kB_{01}\mathrm{e}^{-\mathrm{i}\beta_0 z} \end{bmatrix}. \tag{30}$$

The displacements u_r and u_z of the m-th layer ($1 \leq m \leq n-1$) are

$$\begin{bmatrix} u_r \\ u_z \end{bmatrix} = kQ(r) M_m G_m(z) M_m^{-1} R_m T(m+1,n) \begin{bmatrix} 1 & \mathrm{i}\gamma_{nS} \\ \mathrm{i}\gamma_{nP} & 1 \\ \mathrm{i}\gamma_{nP} & \gamma_n \\ \gamma_n & \mathrm{i}\gamma_{nS} \end{bmatrix} \begin{bmatrix} A_{n2}\mathrm{e}^{\mathrm{i}\alpha_n \sum_{i=1}^{n} h_i} \\ kB_{n2}\mathrm{e}^{\mathrm{i}\beta_n \sum_{i=1}^{n} h_i} \end{bmatrix}, \tag{31}$$

where

$$Q(r) = \begin{bmatrix} -J_1(kr) & 0 & 0 & 0 \\ 0 & J_0(kr) & 0 & 0 \end{bmatrix},$$

$$G_m(z) = \begin{bmatrix} \cos(\gamma_{mP}a) & 0 & -\frac{\sin(\gamma_{mP}a)}{\gamma_{mP}} & 0 \\ 0 & \cos(\gamma_{mS}a) & 0 & -\frac{\sin(\gamma_{mS}a)}{\gamma_{mS}} \\ \gamma_{mP}\sin(\gamma_{mP}a) & 0 & \cos(\gamma_{mP}a) & 0 \\ 0 & \gamma_{mS}\sin(\gamma_{mS}a) & 0 & \cos(\gamma_{mS}a) \end{bmatrix},$$

$$a = k\left(\sum_{i=1}^{m} h_i - z\right). \tag{32}$$

Similarly, the displacements u_r and u_z of the n-th layer (bottom semi-infinite layer) are

$$\begin{bmatrix} u_r \\ u_z \end{bmatrix} = k \begin{bmatrix} -J_1(kr) & 0 \\ 0 & J_0(kr) \end{bmatrix} \begin{bmatrix} 1 & \mathrm{i}\gamma_{nS} \\ \mathrm{i}\gamma_{nP} & 1 \end{bmatrix} \begin{bmatrix} A_{n2}\mathrm{e}^{\mathrm{i}\alpha_n z} \\ kB_{n2}\mathrm{e}^{\mathrm{i}\beta_n z} \end{bmatrix}. \tag{33}$$

With known solutions of A_{n2} and B_{n2}, the displacements are obtained, and they can be used for the evaluation of deformation changes in each layer. The solution of dispersion relation and displacements is obtained, manifesting the existence of the generalized Stoneley wave in a layered structure. Actually, its typical applications are, e.g., borehole logging and data processing in the oil industry, because they are a perfect example of layered structures with the cylindrical formulation and analysis of the generalized Stoneley wave. The current approach is different from other solutions with the Cartesian formulation and the bilayer structure and solutions used in practice. Clearly, it opens up a possibility of improvement because the layers do have an effect on the dispersion relation, as demonstrated in the equations.

3. Numerical examples

3.1. Generalized Stoneley wave in a three-layer structure

As a practical problem close to the Stoneley wave with the cylindrical formulation, the analysis of a generalized Stoneley wave in a layered structure is presented. Since the solutions of Cartesian coordinates are known, it is definitely interesting to make comparisons and visualize the differences in a different coordinate framework. For this objective, two examples of the generalized Stoneley wave in layered structures of elastic solids are provided with numerical solutions of dispersion relation and displacements. Of course, the procedure can be applied to problems of multi-layer structures.

For the confirmation of the existence of the generalized Stoney wave with a layer of elastic solid sandwiched between two semi-infinite elastic solids, the analysis can also be performed to validate the current formulation. The three-layer structure of uniform elastic solids is shown in Fig. 2. The generalized Stoneley wave in such a structure can be easily conceived, since the shrinkage of the thickness of the middle layer will become a typical Stoneley wave problem, such as that appearing in most textbooks. It is expected that the displacements in the two semi-infinite layers will disappear exponentially, as is known to be the case with the standard Stoneley wave. Of course, such a simple case

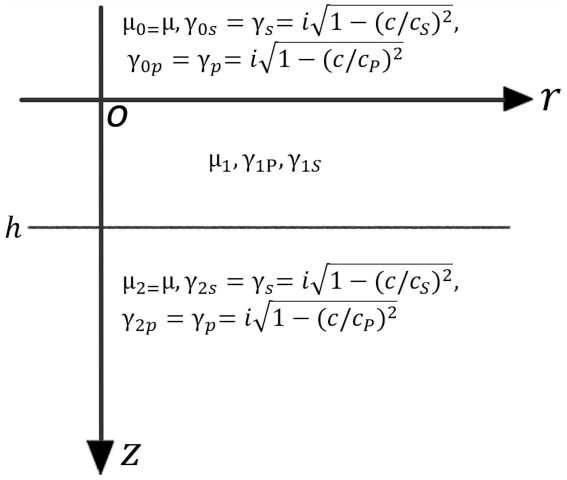

Fig. 2. A three-layer structure for the generalized Stoneley wave with the cylindrical formulation.

of the generalized Stoneley wave is not thoroughly investigated for possible applications, even with the Cartesian formulation. Then, the similar formulation and procedure can be expanded to a structure with multiple finite layers between the two semi-infinite layers, extending the analysis to more practical problems of wave propagation in various engineering applications. Furthermore, the procedure can be modified to analyze a structure with many finite layers.

With the three-layer structure shown in Fig. 2, using the displacement pattern and expressions in the previous section and considering two interfaces at z =0 and $z = h$, the equations of motion take the form

$$\begin{bmatrix}\eta_1 & \eta_2 & \eta_3 & \eta_4 & \eta_5 & \eta_6 & \eta_7 & \eta_8\end{bmatrix}\begin{bmatrix}\Lambda_0(h)\\ \Theta_0(h)\\ kA_{11}\\ kA_{12}\\ k^2B_{11}\\ k^2B_{12}\\ \Lambda_2(h)\\ \Theta_2(h)\end{bmatrix}=\begin{bmatrix}0\\0\\0\\0\\0\\0\\0\\0\end{bmatrix}, \tag{34}$$

where $\Lambda_0(h)$, $\Theta_0(h)$, kA_{11}, kA_{12}, k^2B_{11}, k^2B_{12}, $\Lambda_2(h)$, $\Theta_2(h)$ are amplitudes of displacements, and the matrices of coefficients are

$$\eta_1=\begin{bmatrix}1\\ -\mathrm{i}\gamma_P\\ -\mathrm{i}\gamma_P\mu\\ -\gamma\mu\\ 0\\0\\0\\0\end{bmatrix},\quad \eta_2=\begin{bmatrix}-\mathrm{i}\gamma_S\\ 1\\ \gamma\mu\\ -\mathrm{i}\gamma_S\mu\\ 0\\0\\0\\0\end{bmatrix},\quad \eta_3=\begin{bmatrix}-1\\ \mathrm{i}\gamma_{1P}\\ \mathrm{i}\gamma_{1P}\mu_1\\ -\gamma_1\mu_1\\ \mathrm{e}^{-\mathrm{i}P}\\ -\mathrm{i}\gamma_{1P}\mathrm{e}^{-\mathrm{i}P}\\ -\mathrm{i}\gamma_{1P}\mu_1\mathrm{e}^{-\mathrm{i}P}\\ \gamma_1\mu_1\mathrm{e}^{-\mathrm{i}P}\end{bmatrix},\quad \eta_4=\begin{bmatrix}-1\\ -\mathrm{i}\gamma_{1P}\\ -\mathrm{i}\gamma_{1P}\mu_1\\ -\gamma_1\mu_1\\ \mathrm{e}^{\mathrm{i}P}\\ \mathrm{i}\gamma_{1P}\mathrm{e}^{\mathrm{i}P}\\ \mathrm{i}\gamma_{1P}\mu_1\mathrm{e}^{\mathrm{i}P}\\ \gamma_1\mu_1\mathrm{e}^{\mathrm{i}P}\end{bmatrix},$$

$$\eta_5=\begin{bmatrix}\mathrm{i}\gamma_{1S}\\ -1\\ -\gamma_1\mu_1\\ \mathrm{i}\gamma_{1S}\mu_1\\ -\mathrm{i}\gamma_{1S}\mathrm{e}^{-\mathrm{i}S}\\ \mathrm{e}^{-\mathrm{i}S}\\ \gamma_1\mu_1\mathrm{e}^{-\mathrm{i}S}\\ -\mathrm{i}\gamma_{1S}\mu_1\mathrm{e}^{-\mathrm{i}S}\end{bmatrix},\quad \eta_6=\begin{bmatrix}-\mathrm{i}\gamma_{1S}\\ -1\\ -\gamma_1\mu_1\\ -\mathrm{i}\gamma_{1S}\mu_1\\ \mathrm{i}\gamma_{1S}\mathrm{e}^{\mathrm{i}S}\\ \mathrm{e}^{\mathrm{i}S}\\ \gamma_1\mu_1\mathrm{e}^{\mathrm{i}S}\\ \mathrm{i}\gamma_{1S}\mu_1\mathrm{e}^{\mathrm{i}S}\end{bmatrix},\quad \eta_7=\begin{bmatrix}0\\0\\0\\0\\-1\\ -\mathrm{i}\gamma_P\\ -\mathrm{i}\gamma_P\mu\\ -\gamma\mu\end{bmatrix},\quad \eta_8=\begin{bmatrix}0\\0\\0\\0\\ -\mathrm{i}\gamma_S\\ -1\\ -\gamma\mu\\ -\mathrm{i}\gamma_S\mu\end{bmatrix},$$

$$P=\gamma_{1P}kh, S=\gamma_{1S}kh. \tag{35}$$

At this point, the calculation of dispersion relation and mode shapes requires the vanishing of the determinant of the coefficient matrix of (34). With the transfer matrix method in use with (27), it is obtained that

$$R_1(a{-}b)\begin{bmatrix}\Lambda_0(0)\\ \Theta_0(0)\end{bmatrix}=M_1G_1M_1^{-1}R_1(a{+}b)\begin{bmatrix}\Lambda_2(h)\\ \Theta_2(h)\end{bmatrix},\quad a=\begin{bmatrix}1&0\\0&1\\0&\gamma\\ \gamma&0\end{bmatrix},\quad b=\begin{bmatrix}0&\mathrm{i}\gamma_S\\ \mathrm{i}\gamma_P&0\\ \mathrm{i}\gamma_P&0\\0&\mathrm{i}\gamma_S\end{bmatrix}. \tag{36}$$

After further simplification, the above equation is rewritten as

$$\left(c\boldsymbol{M}_1^{-1}R_1a+dM_1^{-1}R_1b\right)\begin{bmatrix}\Lambda_2(h)-\Lambda_0(0)\\ \Theta_2(h)-\Theta_0(0)\end{bmatrix}+\left(c\boldsymbol{M}_1^{-1}R_1b+dM_1^{-1}R_1a\right)\begin{bmatrix}\Lambda_2(h)+\Lambda_0(0)\\ \Theta_2(h)+\Theta_0(0)\end{bmatrix}=\{0\}, \tag{37}$$

where

$$c=\begin{bmatrix}\cos(P)+1&0&0&0\\0&\cos(S)+1&0&0\\0&0&\cos(P)+1&0\\0&0&0&\cos(S)+1\end{bmatrix}, \tag{38}$$

$$d = \begin{bmatrix} 0 & 0 & -\frac{\sin(P)}{\gamma_{1P}} & 0 \\ 0 & 0 & 0 & -\frac{\sin(S)}{\gamma_{1S}} \\ \gamma_{1P}\sin(P) & 0 & 0 & 0 \\ 0 & \gamma_{1S}\sin(S) & 0 & 0 \end{bmatrix}. \tag{39}$$

From this equation, it is found that $\Lambda_2(h) = \Lambda_0(0), \Theta_2(h) = -\Theta_0(0)$ or $\Lambda_2(h) = -\Lambda_0(0), \Theta_2(h) = \Theta_0(0)$, implying the two displacements are out of phase.

For a numerical calculation, the material properties of the elastic solids are given in Table I, and the dispersion and displacement solutions are shown in Figs. 3 and 4.

In Fig. 3, it can be observed that the Stoneley wave in a three-layer structure exhibits a complex dispersion relation in a wide frequency range. Therefore, from this figure, it can be inferred that at this time, if there is a fundamental mode of the generalized Stoneley wave with a frequency of $f = 3000$ Hz, then its phase velocity is $c = 3494.3$ m/s, and the wavelength is $\lambda = 1.16$ m. There are higher-order wave modes that show the complicated deformation patterns in the structure, but may possess the advantage of rich information about materials and configurations. Using these solutions and parameters, the calculated displacements are shown in Figs. 4 and 5. For the displacement of particles along the longitudinal (z direction), as shown in Fig. 4, there is a significant difference in the

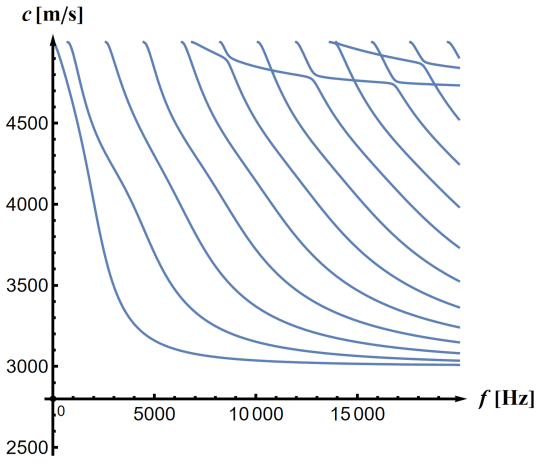

Fig. 3. The dispersion relation of a three-layer structure.

TABLE I

Material properties of the elastic solids in the three-layer structure.

Thickness [m]	Density [kg/m^3]	S-wave velocity [m/s]	P-wave velocity [m/s]
∞	280	5000	8000
1	333.33	3000.02	4698.96
∞	280	5000	8000

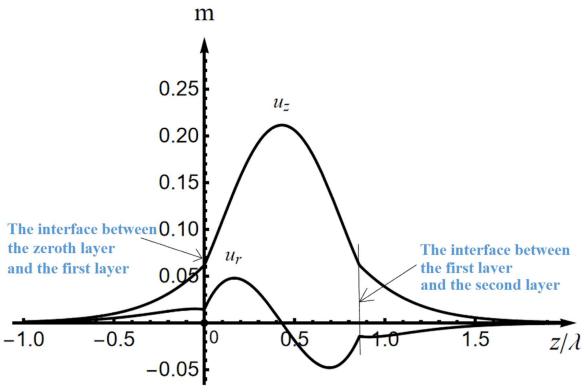

Fig. 4. Variations of displacements u_r and u_z with the depth coordinate z in the three-layer structure.

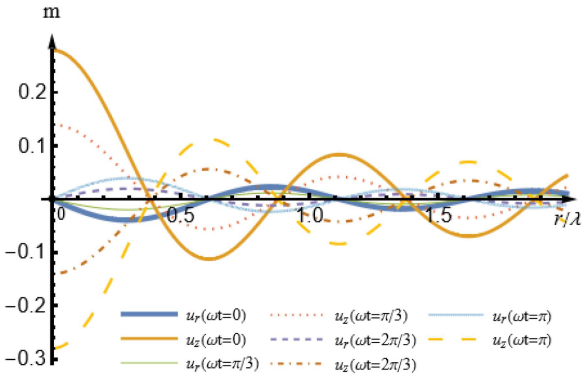

Fig. 5. Variations of displacements u_r and u_z of the interface at $z = 0$.

magnitude and pattern between the semi-infinite layers and the middle layer. The displacements of semi-infinite layers undergo exponential decay, just like the standard Stoneley wave, while in the middle layer, the displacements exhibit simple harmonic oscillation as a bulk wave with two components of similar strength. Regarding the radial variations of displacements, as depicted in Fig. 5, the displacement amplitudes decay rapidly with the radius and then tend to flatten, which is also different from the typical behavior of plane waves. This is different from the Cartesian solutions with constant amplitudes. The reason for such a feature is that the displacement solutions, as given in (33) and earlier studies [11–13], are in the Bessel functions with the cylindrical formulation, which decay with the radius and can eventually be approximated as trigonometric functions with a large radius, while the Cartesian formulation with trigonometric solutions has the constant amplitudes. Of course, the dispersion relations with the two formulations are exactly the same.

Stoneley had proved as early as 1924 that the Stoneley wave is only generated when the medium properties of two semi-infinite solids satisfy specific conditions. However, in the case of generalized Stoneley wave in layered structures, as shown in the examples, the limitation is not needed because the

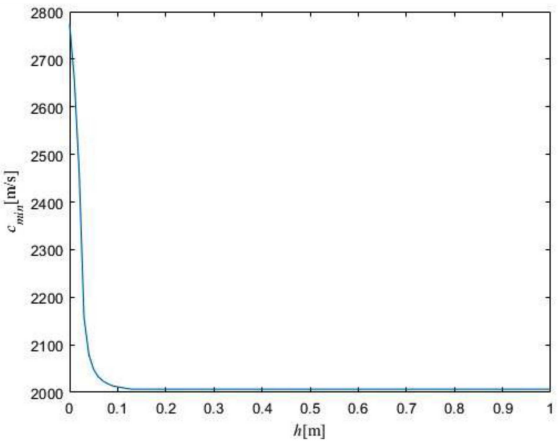

Fig. 6. The phase velocity of the generalized Stoneley wave in the three-layer structure with different thicknesses of the middle layer.

TABLE II

Material properties of elastic solids in the three-layer structure.

Thickness [m]	Density [kg/m^3]	S-wave velocity [m/s]	P-wave velocity [m/s]
∞	19250	2870	5180
h	2500	2000	2500
∞	2700	3100	6300

two semi-infinite solids are not directly in contact with each other, making it possible to generate wave modes close to the ones of Stoneley wave for possible applications in sensing and other functions of layered structures. This can be achieved by changing the thickness of the middle layer in the three-layer structure. For example [17], by calculating the parameters in Table II, we can obtain the phase velocity versus thickness h of the middle layer in the three-layer structure for the generalized Stoneley wave, as shown in Fig. 6. Obviously, when $h = 0$, the wave velocity of the generalized Stoneley wave is equal to the wave velocity of the two-layer standard Stoneley wave, which is 2773 m/s.

3.2. Generalized Stoneley wave in a four-layer structure

We now extend the analytical procedure to a four-layer structure. Table III shows the structure and material parameters of the four-layer model. Figure 7 presents the dispersion curve, and Fig. 8 shows the displacement diagram of the fundamental mode of the generalized Stoneley wave in the four-layer model with a frequency of 2000 Hz, a wave speed of 1630 m/s, and a wavelength of 0.815 m.

Apparently, all the layers, including the semi-infinite ones, will have effects on the phase velocity, and the results can be used for the inverse

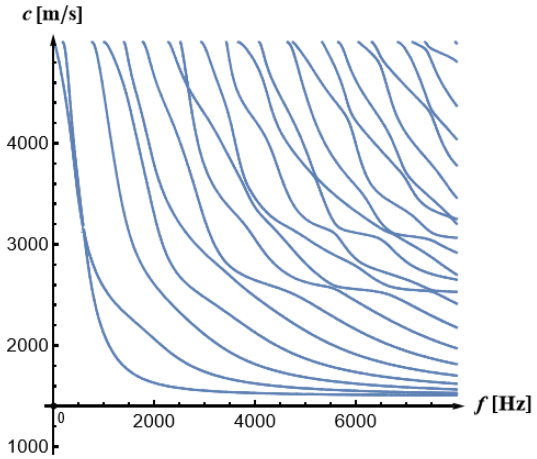

Fig. 7. The phase velocity–frequency curves of generalized Stoneley wave in a four-layer structure.

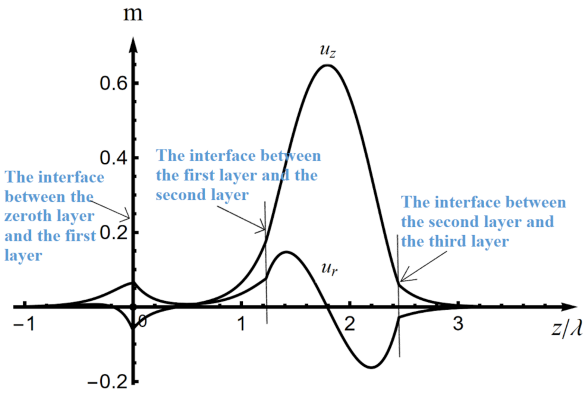

Fig. 8. Displacements u_r and u_z at $r = \lambda$ in the four-layer structure.

TABLE III

Parameters of the structure and materials in the four-layer model.

Thickness [m]	Density [kg/m^3]	S-wave velocity [m/s]	P-wave velocity [m/s]
∞	280	5000	8000
1	333.33	3000.02	4698.96
1	888.9	1500	2500
∞	280	5000	8000

estimation of the material properties, which are important in geological exploration and earthquake studies. This is the advantage of the cylindrical formulation and the layered model of generalized Stoneley wave presented in this study.

4. Conclusions

It is known that using cylindrical formulation to analyze the axisymmetric cylindrical wave has a natural advantage in most cases due to the nature

of the point excitation and some structural configurations. In this analysis, it is found that in a horizontally layered structure, the generalized Stoneley wave does exist with the signature pattern of exponential decay in the depth of the semi-infinite solids. Furthermore, the decaying of displacement amplitudes with radius is also a feature distinct from the cylindrical formulation but is not widely noticed. Clearly, all these properties are closely related to the analytical results and, more importantly, to the estimation of material properties and excitation for the determination of geological structures in relation to critical applications. It is believed that the utilization of the analytical procedure presented in this study will provide different results from the Cartesian formulation and that they can be used as mutual references for the refined characterization of targeted structures. Similar applications in nondestructive testing and healthcare can also take the same approach to alternative results to enhance the assurance mechanism.

Author's contributions

The paper was conceived, revised, and submitted by JW. The mathematical formulation, procedure, derivation, calculation, and check were made by BWY with the help of HMJ. Reviews and discussions of the study, results, and drafting were also completed with the participation of JW and BWY. All authors have read and agreed to the published version of the manuscript. The data of this study are available from the authors and the authors' websites.

The funders and other parties had no role in the design of the study, in the collection, analyses, or interpretation of data, in the writing of the manuscript, or in the decision to publish the results.

Acknowledgments

This research is supported by the National Natural Science Foundation of China (Grants 11672142, 52278189, and 51878606), Zhejiang Province Basic Public Welfare Research Project (Grant LGG22E080007), the Ningbo City Transportation Science and Technology Project (Grants 202116 and 202207), and with additional support through the Technology Innovation 2025 Program (Grant 2019B10122) of the Municipality of Ningbo, Zhejiang, China.

References

[1] R.E. Sheriff, *Encyclopedic Dictionary of Applied Geophysics* Society of Exploration Geophysicists, 2002.

[2] R. Stoneley, *Proc. R. Soc. Lond. A* **106**, 416 (1924).

[3] S.V. Kuznetsov, *Z. Angew. Math. Phys* **71**, 114 (2020).

[4] O. Onen, Y.C. Uz, *Phys. Proc.* 70, 217 (2015).

[5] S.V. Kuznetsov, *Int. J. Mech. Mater. Design* **17**, 601 (2021).

[6] J.G. Scholte, *Geophys. Suppl. Mon. Not. R. Astron. Soc.* **5**, 120 (1947).

[7] W.T. Thomson, *J. Appl. Phys.* **21**, 89 (1950).

[8] N.A. Haskell, *Bull. the Seismol. Soc. Am.* **43**, 17 (1953).

[9] J.W. Dunkin, *Bull. the Seismol. Soc. Am.* **55**, 335 (1965).

[10] L. Knopoff, *Bull. the Seismol. Soc. Am.* **54**, 431 (1964).

[11] C. Bian, J. Wang, B. Huang, L. Xie, L. Yi, L. Yuan, H. Li, Y. Tian, *Phys. Scr.* **96**, 125272 (2021).

[12] C. Bian, J. Wang, L. Xie, Y. Zhang, H. Li, Y. Tian, *Arch. Appl. Mech.* **92**, 649 (2022).

[13] Ji Wang, S. Wang, L. Xie, Y. Zhang, L. Yuan, J. Du, H. Zhang, *Theor. Appl. Mech. Lett.* **10**, 120 (2020).

[14] B. Xiao, C. Li, *Chinese J. Eng. Geophys.* **1**, 38 (2004) (in Chinese).

[15] Y. Chen, J. Liu, J. Wang, T. Maa J. Du, H. Li, *Acta Phys. Pol. A* **140**, 105 (2021).

[16] K.F. Graff, *Wave Motion in Elastic Solids* Dover Publications, 1975.

[17] C. Bian, B. Huang L. Xie, L. Yi, L. Yuan, J. Wang, *Acta Phys. Pol. A* **139**, 124 (2021).